The effect of grain size on the twin initiation stress in a TWIP steel

K.M. Rahman[a], V.A. Vorontsov[a], D. Dye[a]

[a]*Department of Materials, Royal School of Mines, Imperial College London, Prince Consort Road, London SW7 2BP, UK*

Abstract

The influence of grain size on the twinning stress of an Fe-15Mn-2Al-2Si-0.7C twinning induced plasticity (TWIP) steel has been investigated. Five grain sizes were obtained using a combination of cold rolling and annealing. Electron backscatter diffraction (EBSD) analysis revealed that the material exhibited a typical cold rolled and annealed texture. Tensile testing showed the yield stress to increase with decreasing grain size, however, the ductility of the material was not substantially affected by a reduction in grain size. Cyclic tensile testing at sub-yield stresses indicated the accumulation of plastic strain with each cycle, consequently the nucleation stress for twinning was determined. The twin stress was found to increase with decreasing grain size. Furthermore, the amount of strain accumulated was greater in the coarser grain material. It is believed that this is due to a difference in the twin thickness, which is influenced by the initial grain size of the material. SEM and TEM analysis of the material deformed to 5 % strain revealed thinner primary twins in the fine grain material compared to the coarse grain. TEM examination also showed the dislocation arrangement is affected by the grain size. Furthermore, a larger fraction of stacking faults was observed in the coarse-grained material. It is concluded that the twin nucleation stress and also the thickness of the deformation twins in a TWIP steel, is influenced by the initial grain size of the material. In addition grain refinement results in a boost in strength and energy absorption capabilities in the material.

Key words: Twinning, Grain Size, Austenitic Steel, Yield Phenomena, Annealing

1. Introduction

High manganese Twinning Induced Plasticity (TWIP) steels have been attracting significant research interest in recent years owing to their high strength (up to 800 MPa) and superior formability (up to 95 % ductility) [1, 2, 3, 4]. These excellent characteristics arise from a high work hardening capacity in the steel, which is due to the continuous formation of mechanical twins during deformation. Hence, these properties make the alloys ideal candidate materials for energy absorption applications, including military vehicle armour and automotive crash safety. However, the widespread use of TWIP steels, particularly for automotive applications, has been limited. This is partly due to their relatively low yield strength, when compared to other advanced high strength steels (AHSS).

The TWIP mechanism is observed in alloys which have a medium stacking fault energy (SFE), typically in the range of 18-45 $\mathrm{mJ\,m^{-2}}$ [5, 4] and is characterised by the formation of discrete sheared grain subregions containing a mirror plane at the interface, *i.e.* nanometer thick deformation twins. The impressive strain hardening exhibited in TWIP steels is largely attributed to a dynamic Hall-Petch effect [6, 7, 8]. As deformation progresses and twins nucleate, they act as obstacles for gliding dislocations, effectively resulting in a continuous grain refinement process. Consequently, this leads to a reduction in the dislocation mean free path, thus producing the characteristic high hardening rate observed. Although several mechanisms have been proposed to explain the formation of deformation twins [7], it is generally considered to be a process which proceeds *via* a dislocation mechanism, whether by a pole mechanism [9], a deviation process [10], or by twin nucleation through the formation of stacking faults [11].

The stress required to generate twinning, known as the 'twinning stress', can be considered to be a combination of two separate terms. Firstly, a stress is required for twin nucleation followed by a further stress for twin growth, together defining the twinning stress. However, determining the stress required to nucleate a twin experimentally is extremely difficult [12]. Consequently, it is generally considered that the nuclei for twins already exist within the material *e.g.* stacking faults, and that the twinning stress which is experimentally determined is actually the stress required for twin growth.

The morphology and thickness of deformation twins is controlled by the SFE as proposed by Friedel [13], which has been extended by Allain *et al.* [14] who defined a linear relationship between SFE and twin thickness. Similarly, twin thickness is also affected by the initial grain size of the material [14]. Once the first twin system is activated, the twins must develop through the whole grain. However, once secondary twin systems become active, the twins only need to develop between one twin boundary to another since twin boundaries are strong obstacles and comparable to grain boundaries. Thus, secondary twins are much thinner than the primary twins and larger grain sizes promote the growth of thicker primary twins.

The relatively low yield strength of TWIP steels has been an obstacle inhibiting the widespread use of the alloys in industrial applications. However this problem can be resolved using a range of methods. Precipitation strengthening is one such method. However, the high concentration of carbon, which is generally alloyed into TWIP steels, can lead to the formation of carbides. Furthermore, for longer annealing periods the formation of pearlite can occur [6]. Another method available for improving the strength of an alloy is grain refinement. This is attractive since it does not involve changing the chemical composition of the material. Bouaziz *et al.* [6] have predicted that a yield stress of 700 MPa can be obtained in an Fe-22Mn-0.6C TWIP steel with a grain size of ∼1 μm. Similarly, Santos *et al.* [15] and Kang *et al.* [16] have investigated the effect of annealing temperature on recrystallisation in TWIP steels, concluding that specimens exhibiting a finer grain size also display higher yield strengths.

Deformation twinning is strongly dependent on crystallographic grain orientation and the average grain size of the material [17, 18]. However, only a few studies have been conducted which investigate the influence of grain size on the strain hardening and twinning behaviour in TWIP steels [19, 18, 20, 21, 22]. Gutierrez-Urrutia *et al.* [19] have attempted to elucidate the role of grain size on the strain hardening behaviour of a TWIP steel by investigating the dislocation and twin substructures in the material using electron channeling contrast imaging (ECCI). The authors concluded that the fine-grained material investigated exhibited a different hardening behaviour compared to the coarse-grained material. This behaviour is explained by the existence of a loose dislocation arrangement in the fine-grained material compared to a cell block structure in the coarse-grained. This leads to the formation of a single twin type, lamellar twin structure in the fine-grained material and a multiple twin substructure in the coarse-grained consisting of two active twin types.

In a separate study, Gutierrez-Urrutia *et al.* [18] found that grain refinement within the micrometer range does not suppress deformation twinning, although it does become more difficult and a reduction in twin area fraction occurs in the finer grain material. The authors also found that a Hall-Petch relation provided a good estimate for the effect of grain size on the twinning stress and the experimental evidence suggested that the effect of the grain size on twinning stress was similar to the effect on the yield stress of the material. However, Ueji *et al.* [21] suggest that deformation twinning is strongly suppressed by grain refinement. The contrasting conclusions from the two studies may be due to the influence of the stacking fault energy of the alloys investigated in each study. Gutierrez-Urrutia *et al.* [18] used an alloy with a low stacking fault energy ($\sim 24\,\mathrm{mJ\,m^{-2}}$ [23, 24, 25]), whereas Ueji *et al.* [21] utilised a material alloyed with aluminium and silicon, which had a higher SFE ($\sim 42\,\mathrm{mJ\,m^{-2}}$).

Bouaziz *et al.* [22] have studied the effect of grain and twin boundaries on the hardening mechanisms of TWIP steels, with particular emphasis on the Bauschinger effect during reverse strain testing. Here the authors concluded using a physically based model that the twin nucleation stress was independent of the grain size and was approximately 550 MPa for the grain sizes investigated (between 1.3 - 25 μm). They consequently inferred that the twin initiation strain increased with grain size and was 12 % true strain for a 25 μm grain size.

A complimentary study by the authors on a TWIP steel using X-ray synchrotron diffraction measurements has shown evidence of the nucleation of deformation twins before the macroscopic yield point of the material. This observation was rationalised using *ex-situ* cyclic tensile testing at stresses below the macroscopic yield stress. The accumulation of strain with each cycle was observed and post deformation microscopy revealed the presence of fine deformation twins in the sample.

In the present work, the effect of austenite grain size on the hardening behaviour and twin initiation stress of a TWIP steel has been investigated by performing a variety of tensile tests. A range of grain sizes has been obtained by varying annealing time. The effect of grain size on the mechanical properties and hardening behaviour has been determined and the twin initiation stress has been investigated using cyclic tensile testing. Finally, the mechanical testing results have been rationalised and augmented using a range of microscopy techniques.

2. Experimental Procedures

2.1. Material

The TWIP steel used in this study had a nominal composition of 15Mn-2Al-2Si-0.7C wt. % and was provided in 3 mm rolled sheet form by Tata Steel Strip Mainland Europe. The average grain size of the material was 10 $\pm$ 6 µm and the stacking fault energy was calculated to be 30 $\pm$ 10 mJ m^{-2} using thermodynamics based models and data [23, 24, 25].

2.2. Cold rolling and annealing procedure

Strips measuring 25$\times$80 mm were cold rolled parallel to the rolling direction of the as-received plate at $\sim$10 % reduction per pass to a final thickness reduction of 50 %; thereby achieving a 1.5 mm final strip thickness.

In order to obtain a range of grain sizes the strips were annealed at 850 °C, employing different soaking times in the furnace to achieve the final grain sizes. Samples were subsequently either quenched in cooled brine, water or were air cooled. The experimental annealing schedule is summarised in Table 1.

Table 1: Annealing schedule used to obtain different grain sizes from the cold rolled TWIP steel.

Sample	Annealing temp (°C)	Annealing time (min/h)	Cooling conditions
1	850	1 min	-20 °C, brine quench
2	850	2 min	Water quench
3	850	24 h	Air cool
4	850	96 h	Air cool

2.3. Microscopy

Samples for light microscopy (LM) and electron backscatter diffraction (EBSD) were prepared following a standard metallographic schedule. Specimens for LM were etched using a solution of 4 % Nital to reveal the grain boundaries.

EBSD was performed for grain size analysis on a JEOL JSM6400 SEM fitted with an Oxford Instruments HKL Nordlys EBSD detector. Step sizes ranging between 0.15-1 µm were selected for indexing. Backscattered imaging of the fine twins was conducted on a Zeiss Auriga FEGSEM. Samples for transmission electron microscopy were prepared using Focussed Ion Beam (FIB) milling on a FEI Helios NanoLab 50 series DualBeam microscope and TEM examinations were conducted on a JEOL 2000FX microscope.

2.4. Texture

After cold rolling and annealing, the texture was characterised from EBSD measurements where a minimum of 1000 grains had been indexed. The data was then used to reconstruct a complete orientation distribution function (ODF) using spherical harmonics. A Williams-Imhof-Matthies-Vinel (WIMV) [27] calculation was then performed to remove any 'ghost' points. This involves fitting a minimum-curvature orientation distribution (based on the weight of each Euler angle triplet) to the spherical harmonics pole figure. The WIMV calculated ODF is then used to reconstruct the final set of experimental pole figures. These are then visualised using the software Pod2k. The WIMV calculated ODF is also used to determine the texture index (TI). The texture index is useful parameter to compare the texture strength of a sample without regard for the individual components of that texture, where the TI is the mean square value of the orientation distribution. Therefore, a random material has a TI equal to unity, while textured samples have higher values.

2.5. Tensile testing

Tensile testing was conducted on a Zwick Roell 100 kN load frame using a 10 mm gauge length extensometer. Testing was conducted at a nominal strain rate of $10^{-3}\,\mathrm{s}^{-1}$ on samples with gauge dimensions of $19\times1.5\times1.5$ mm. The tensile axis was aligned to the rolling direction of the plate.

2.6. Cyclic testing and twin stress determination

In a complimentary study by the authors evidence was provided using multiple methods that twinning was occurring at sub yield stresses, this included X-ray synchrotron lattice strain, peak width and intensity evolution in addition to *ex-situ* cyclic tensile testing.

Since it has been shown that the current experimental TWIP steel twins at stresses below the macroscopic yield point, it is possible to experimentally determine the twin initiation stress for various grain sizes using a series of cyclic tensile tests at different target stresses which are below the yield stress. The total accumulated strain (ε_t) can be determined after a set number of loading cycles (N). This can then be used to calculate the amount of microstrain induced per cycle (ε_{cycle}) for a given target stress, *i.e.* $\varepsilon_{cycle} = \varepsilon_t/N$. Once the accumulated strain at different stresses is determined for each sample, a linear relationship can be used to determine the twin initiation stress.

Cyclic testing was conducted between a threshold stress of 10 MPa and a selected target stress for 50 cycles. The initial target stress was 100 MPa, this value was increased by an additional 100 MPa upon completion of every 50 cycles up to the yield stress for each experimental sample. Each test was conducted on separate tensile specimens with gauge dimensions of $19\times1.5\times1.5$ mm, the tensile axis was aligned to the rolling direction of the plate. Testing was conducted under position control at a nominal strain rate of $10^{-3}\,\mathrm{s}^{-1}$. The accumulation of permanent strain per cycle was also confirmed using samples with strain gauges bonded on for extension measurements instead of an extensometer.

3. Results and Discussion

3.1. Microstructure characterisation

The microstructure of the test material after cold rolling and annealing was fully austenitic for all the experimental annealing times. Electron backscatter diffraction (EBSD) revealed the existence of numerous $\Sigma 3$ annealing twins. However, no evidence of ϵ-martensite was found, Figure 1(a-e). EBSD was also used to determine the average grain size, Figure 1(f). Here twin boundaries were excluded from the grain size analysis. The cumulative distribution function (CDF) from the raw EBSD data was smoothed using a Weibull fitting function. Subsequently, the final number average grain size distribution function was obtained from the derivative of the Weibull function.

A unimodal grain size distribution was observed in all the samples (Appendix), Figure 1(f), and average grain sizes between 0.7 - 84 μm were obtained

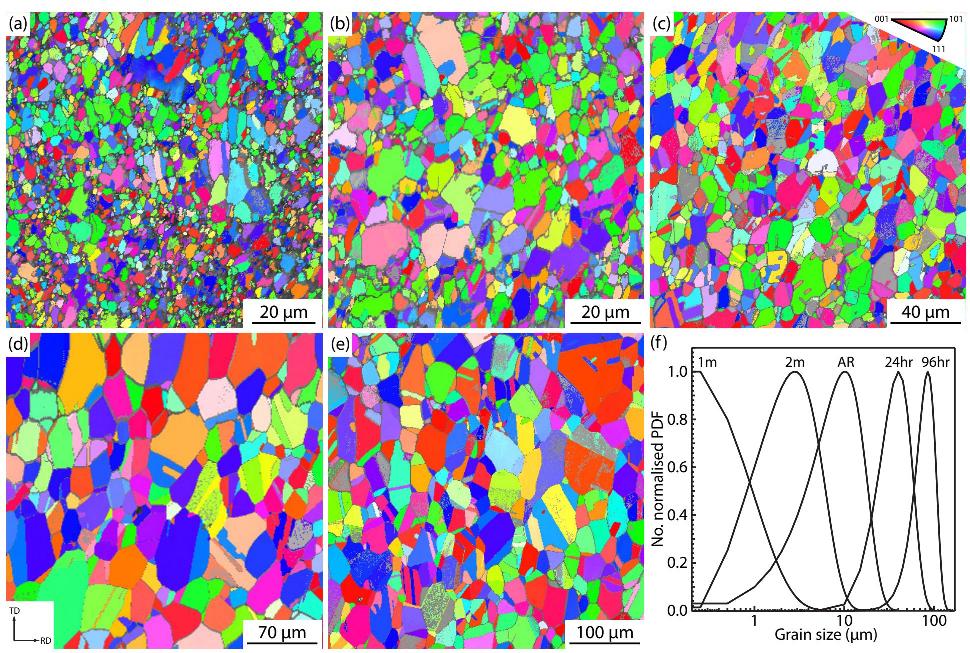

Figure 1: EBSD maps with IPF colouring relative to the rolling direction of specimens cold rolled to 50 % reduction and annealed for; (a) 1 min followed by brine quench [84 % indexing], (b) 2 min then water quench [88 % indexing], (c) as-received material [85 % indexing], (d) 24 h then air cooled [92 % indexing] and (e) 96 h air cooled [88 % indexing]. Number average grain size distribution smoothed using a Weibull fitting function (f).

using the different annealing schedules, Table 2. The experimental steel had an average grain size of 10 µm in the as-recieved material condition. Therefore, this sample was not subjected to additional cold rolling and annealing.

Table 2: Average grain size determined from EBSD after cold rolling to 50 % reduction and annealing at 850 °C.

Sample	Annealing time (min/h)	Cooling conditions	Scan Area (µm)	No. of Sampled Grains	Average grain size (µm)
1	1 min	-20 °C, brine quench	50 × 50	1571	0.7 ± 0.5
2	2 min	Water quench	200 × 150	1077	4.3 ± 2.4
AR	——	——	500 × 500	1683	10 ± 6.0
3	24 h	Air cool	2500 × 1500	1320	45 ± 2.0
4	96 h	Air cool	2500 × 2500	1142	84 ± 1.0

The texture of the investigated alloy after cold rolling and annealing was determined using EBSD after a minimum of 1000 grains were indexed, Figure 2. A typical cold rolled and annealed texture is exhibited, consisting of three main components *i.e.* Brass, Goss and Copper. The annealed and recrystallised texture is similar to that which would be expected in a cold rolled sample [28] with the exception of weakening of the texture intensities. Since the recrystallised texture shares the main components to a typical cold rolled f.c.c. texture, it may indicate that recrystallisation occurs *via* a site saturated nucleation mechanism as suggested by Bracke *et al.* [28]. The texture seen in Figure 2(AR) is weak and is essentially random texture. This is the 10 µm grain size specimen which is tested in the as received material condition, and has not been further cold rolled and annealed. Retention of cold rolling texture does not always occur and randomisation is possible. This may be due to the fragmentation of coarse grains during cold rolling and the profuse formation of annealing twins, particularly at higher annealing temperatures.

3.2. Mechanical characterisation

The tensile behaviour of the five grain sizes investigated in this study can be seen in Figure 3(a). A significant influence of grain size on the yield strength of the steel is clearly seen and, as expected, the yield strength increases with decreasing grain size. Similarly, an increase in the ultimate tensile strength (UTS) is exhibited with decreasing grain size. However, an interesting observation is that the elongation to failure for all the experimental samples is relatively similar and a decreasing grain size appears to have little effect on the strain to failure. It has been reported elsewhere [29] that although high stacking fault energy (SFE) f.c.c. and b.c.c. alloys tend to display high yield strengths with a reduced grain size such as 1 µm, they also tend to exhibit a substantial loss in ductility. The observations in the experimental material may be ascribed to the relatively low SFE of the alloy and also due to a minor influence on deformation twinning caused by a reduced grain size.

A remarkably high strain hardening rate is observed for all the grain sizes investigated, which is characteristic of f.c.c. steels which deform *via* twinning. However, the hardening behaviour of the material is also affected by the grain

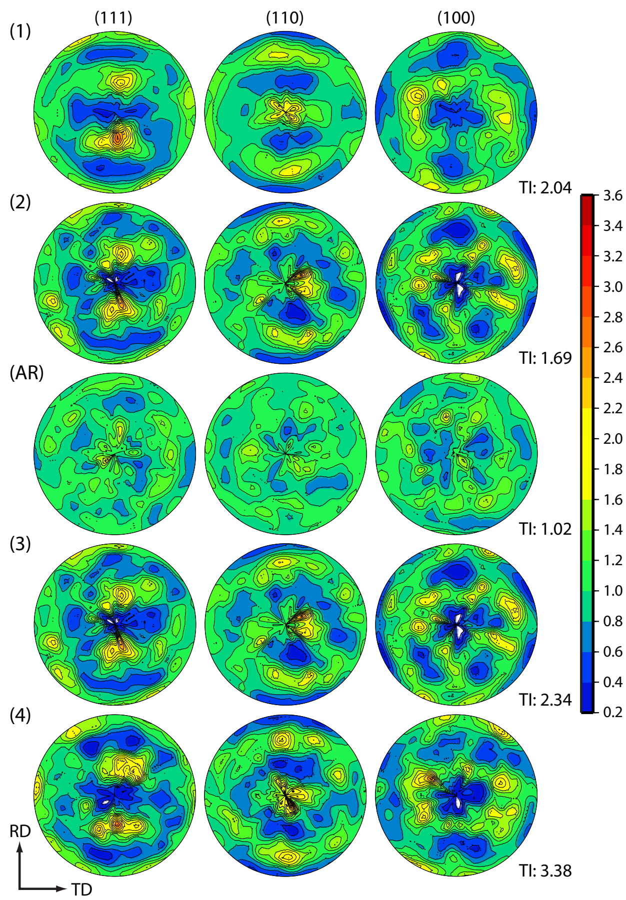

Figure 2: Characteristic cold rolled and annealed texture determined using EBSD for the different annealing conditions along with the texture index (TI); (1) 0.7 μm material, (2) 4.3 μm, (AR) 10 μm material in the as-received condition, (3) 45 μm and (4) 84 μm grain size TWIP steel.

size where an extra work hardening region is exhibited in the hardening curve of the fine grain (FG) specimens *i.e.* 0.7 and 4.3 μm when compared to the three hardening regimes exhibited by the coarse grain (CG) material, Figure 3(b).

The hardening behaviour exhibited by the fine grain material initiates with a decrease in the hardening rate with the onset of straining (region 1). The decrease in hardening observed in region 1 is non-linear. This suggests a non-equilibrium between the accumulation and recovery of dislocations. The consequent implication is that a certain level of strain is required before the deformation twins being formed are thick and frequent enough to affect the hardening rate. The first stage of the hardening behaviour extends to a minimum with further strain, finally transiting to region 2. Region 2 initiates with an increase in the hardening rate. This is caused by an increase in the deformation twinning

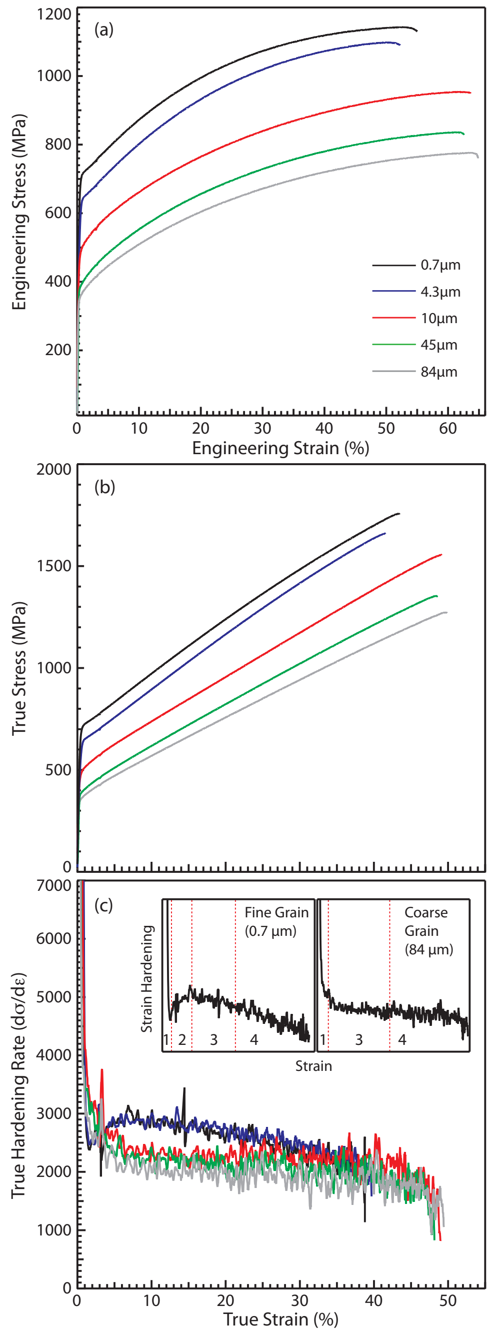

Figure 3: Influence of grain size on the mechanical behaviour of the experimental TWIP steel. (a) engineering stress-strain response, (b) true stress-strain behaviour and strain hardening behaviour.

rate. Furthermore, it has been suggested that the increase in the hardening rate may be due to the activation of secondary twin systems [30, 31]. The second hardening stage extends to a maximum after which the third region in the hardening behaviour begins. Region 3 extends to higher strains ($\sim$30 % strain) and proceeds over a larger strain window compared to regions 1 and 2. As region 3 extends with further straining, a subtle and gradual decrease in the gradient of the hardening rate is observed ($\sim$30 %), which leads to the onset of region 4. Region 4 continues with a decrease in the work hardening rate until the UTS is reached. The initial decrease in the hardening rate is likely to be caused by a reduction in the twinning activity. Since previously formed twins will now be present in the microstructure, they will have effectively reduced the grain size of the material. Therefore, higher stresses will be required to generate further twins. As deformation progresses, the twin volume fraction will inevitably increase and consequently the twin bundles will become denser and thicker. The fraction of newly twinned grains will saturate and the nucleation of new twins will become more difficult in the already strain hardened parent grains. Any grains which remain free of twins will almost certainly be in an orientation which is unfavourable for deformation twinning. Hence, a high work hardening rate cannot be maintained with further strain and, as a consequence, a gradual decrease in the hardening rate is observed until fracture.

The hardening behaviour exhibited by the coarse grain specimens demonstrates only three distinct work hardening regions compared to the four seen in the fine grain material *i.e.* region 2 is not observed in the coarse grain hardening behaviour. Instead, a gradual decrease in the hardening rate is observed directly between region 1 and region 3. Similar to the fine grain behaviour, a delicate change in the hardening rate at higher strains ($\sim$25 % strain) is observed *i.e.* a transition between region 3 and 4. However, the reduction in the hardening rate between regions 3 and 4 ($\sim$50 %) is more defined when compared to the transition seen in the fine grain behaviour. The hardening behaviour demonstrated by the coarse grain material is often observed in partially recrystallised microstructures. In such cases, an increase in the hardening rate during early deformation is not observed due to the difficulty of twin formation in the recovered microstructure [15]. However, since the samples investigated in this study are fully recrystallised, the lack of increasing hardening rate during the early deformation may be due to the need for a longer strain window in order to saturate the larger grains with a sufficient volume fraction of deformation twins compared to the fine grain material. Thus an increase in hardening rate is not observed. A further cause for the hardening behaviour observed may be due to a lower primary deformation twinning rate in the coarser grain material. Idrissi *et al.* [32] have also reported different hardening behaviours observed for TWIP steels with different chemical compositions. The authors suggested that the different hardening rates were resultant of different thickness sessile dislocations which are stored at the twin-matrix interface. In addition, the twins formed in the grain sizes showing an extra hardening region were thinner and contained a larger density of sessile defects, thus making the twins stronger. Therefore, the different hardening behaviour observed in the current study may arise due to a difference in twin thickness, which is influenced by the grain size.

The increase in the strength of the material with decreasing grain size is well represented by a Hall-Petch type relation:

$$\sigma_y = \sigma_0 + \frac{K^{HP}}{\sqrt{D}} \tag{1}$$

where σ_y is the yield stress, σ_0 is the lattice friction stress, K^{HP} is the strengthening coefficient and D is the grain size, Figure 4. It can be seen from Figure 4 that the experimental values are consistently higher than the predicted behaviour using values for the Hall-Petch constants from the literature for a Fe-22Mn-0.6C TWIP steel ($\sigma_0 = 132\,\mathrm{MPa}$ and $K^{HP} = 449\,\mathrm{MPa\,\mu m^{1/2}}$) [6, 33]. This would suggest that the addition of aluminium and silicon in the present experimental alloy has a significant strengthening influence on the alloy. This will also alter the SFE and consequently the morphology of the deformation twins. Thus, using Hall-Petch constants fitted for the experimental data ($\sigma_0 = 305\,\mathrm{MPa}$ and $K^{HP} = 330\,\mathrm{MPa\,\mu m^{1/2}}$) shows a better agreement with the experimental observations.

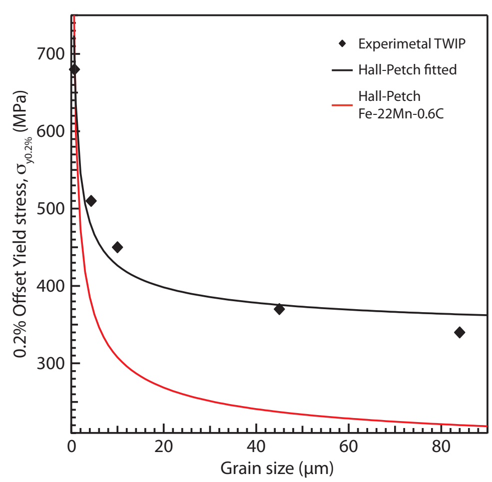

Figure 4: Influence of grain size on the yield strength of the material can be represented using a Hall-Petch type relationship. The addition of silicon and aluminium in the experimental steel suggests additional strengthening (black line) compared to an FeMnC TWIP steel (red line).

3.3. Influence of grain size on twin stress

Cyclic tensile testing revealed that an accumulation of plastic strain occurred with each tensile cycle at selected stresses, which were below the yield stress of the test specimen. This is illustrated in Figure 5, which shows the accumulation of strain in the 10 μm grain size material, this behaviour was exhibited by all the different grain size specimens investigated. The stress at which the accumulation

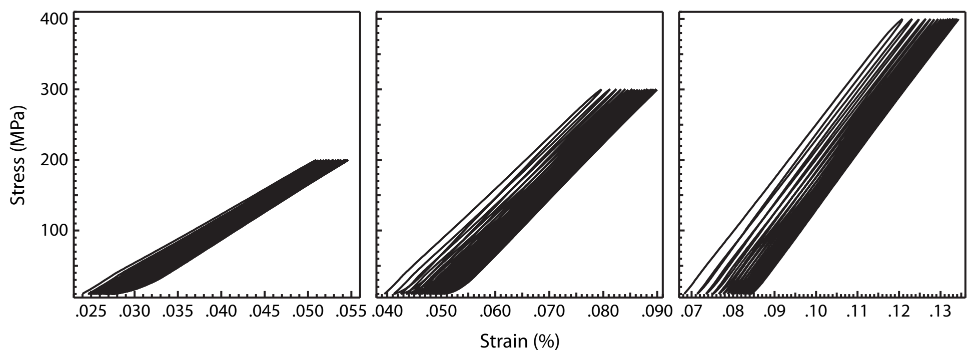

Figure 5: Accumulation of permanent strain during cyclic tensile testing at a range of stresses below the yield point is exhibited as shown in the 10 μm grain size material. This behaviour is characteristic of all the experimental grain sizes.

of strain initiated was lower in the coarse grain material, which suggests that a coarse grain size promotes early deformation twinning.

The twin initiation stress was calculated by plotting the strain accumulated per cycle at different stresses, fitting a linear relationship to the experimental data and finding the intercept, Figure 6. The results indicate that grain size refinement increases the twin initiation stress in the material, Table 3. Furthermore, less strain is accumulated in the fine grain material compared to the coarse grain which suggests that grain refinement suppresses either the formation of twins or the subsequent thickening of the nucleated twins. Using the experimentally determined twin stress for each grain size, it is possible to estimate the critical twin stress for twin nucleation at the single crystal limit (*i.e.* $1/d = 0$). This is achieved by plotting the twin initiation stress against the reciprocal square root of the grain size. Fitting a linear relationship to the data enables the limit of large grain size to the twin stress to be calculated, Figure 7(a). The experimental data suggests the critical twin nucleation stress for an infinite grain size to be $\sim$50 MPa.

It is generally accepted that twinning in pure metals and alloys is initiated by pre-existing dislocations that dissociate into multi-layered stacking faults which creates a twin nucleus. Several dislocation based models have been proposed for twin nucleation in f.c.c. materials [34, 35, 11]. All involve the glide of

Table 3: Calculated twin initiation stress for different grain sizes.

Sample	Average grain size (μm)	Twin Stress (MPa)	0.5 % Yield Stress (MPa)
1	0.7 ± 0.5	316	720
2	4.3 ± 2.4	184	640
AR	10 ± 6.0	115	490
3	45 ± 2.0	77	390
4	84 ± 1.0	62	350

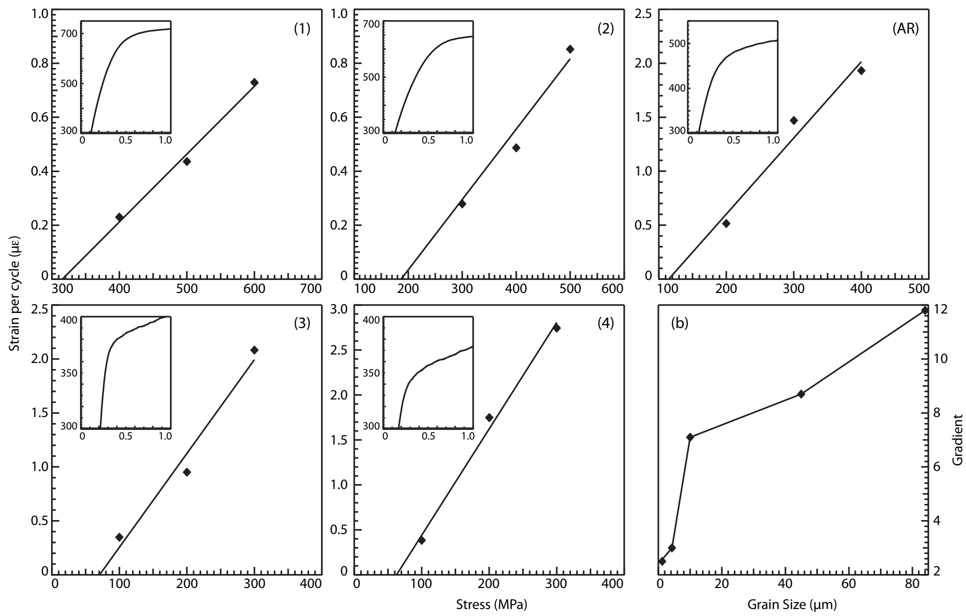

Figure 6: Twin initiation stress determined by plotting accumulated strain against stress and fitting a linear relationship to the experimental data along with a close view of the macroscopic yield transition (inset). (1) 0.7 μm grain size material, (2) 4.3 μm, (AR) 10 μm as-received material, (3) 45 μm and (4) 84 μm and (b) influence of grain size on the gradient of the fitted lines seen in (1-4).

Shockley partial dislocations with Burgers vector $a/6\langle 112\rangle$ on successive $\{111\}$ planes. Since twinning is influenced by the SFE, Venables [35] proposed a phenomenological relationship between the SFE and the twinning stress where the influence of the SFE on the twinning stress is propotional. Bases on the analysis of several f.c.c. metals and alloys Narita and Takamura [36] determined that the SFE and twin stress were proportional such that

$$\tau_{twin} = \frac{\gamma_{SF}}{K b_s} \tag{2}$$

where τ_{twin} is the critical resolved shear stress to separate a leading Shockley partial from the trailing partial and thus create a twin, γ_{SF} is the stacking fault energy, K is a fitting parameter which was determined to be 2 by Narita and Takamura [36] and b_s is the Burgers vector for a Shockley partial dislocation.

Since τ_{twin} can be considered to be the twinning stress for a single crystal, Equation 2 can be used to calculate a critical twinning stress for the experimental alloy using the SFE of the material. Considering the standard deviation which arises from the thermodynamic derivation of the SFE in the experimental alloy, a critical twin stress as low as ∼67 MPa is predicted. The calculated stress is remarkably close to the experimental prediction for the critical twin stress for the single crystal limit.

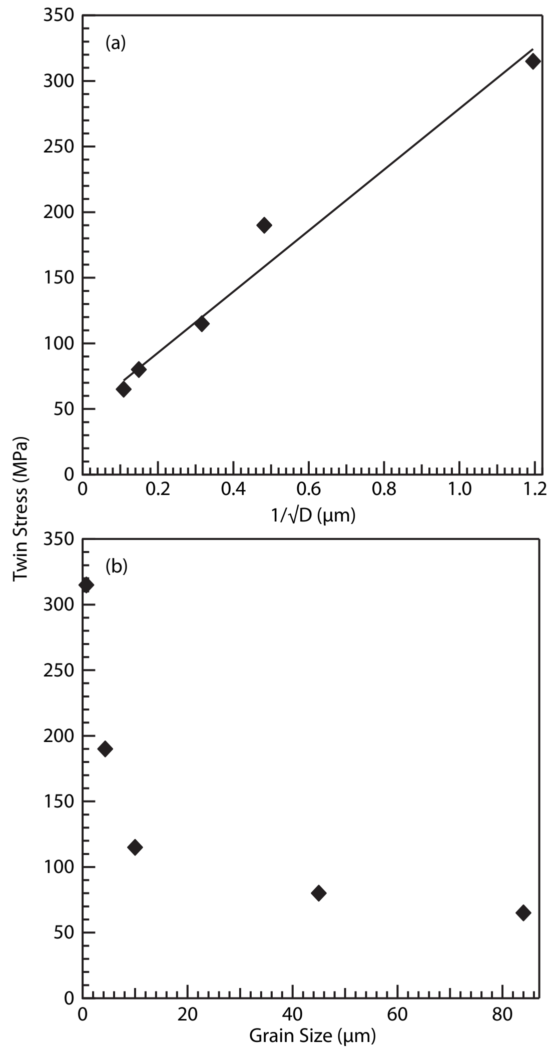

Figure 7: (a) Critical twin initiation stress for an infinite grain size TWIP steel determined from experimental data and (b) effect of grain size on the twin initiation stress shows a Hall-Petch type behaviour.

It should be noted that such phenomenological relations are limited. Therefore, a degree of uncertainty is expected. Kibey *et al.* [37] have shown that the true twinning stress depends on the entire generalised planar fault energy, including the unstable twin stacking fault energy and not just the intrinsic stacking fault energy. Similarly, Meyers *et al.* [38] have discussed how the equation proposed by Venables [35] does not always predict the twin stress correctly, even though the relationship is accurate for most f.c.c. metals. An example of this is the case of some copper alloys for which the twin stress varies with the square root of the SFE.

The deformation and strain hardening behaviour of low SFE materials is strongly influenced by grain size and consequently the twin stress is dependent on the initial grain size of the material. The length scale of twinning is also expected to have a significant effect on the twinning stress which, in turn, is also affected by the length scale for homogeneous slip. It has been shown by El-Danaf *et al.* [39] that the average slip length during straining in low SFE large grain f.c.c. metals does not change significantly. However, in fine grain materials the average slip length decreases with strain. Although these reductions are relatively small, it is nevertheless enough to inhibit the build up of sufficient dislocations that are necessory to nucleate a nano-sized twin. Furthermore, a low SFE in f.c.c. materials hinders the development of in-grain misorientations. This allows the slip length to remain close to initial grain size, *i.e.* before deformation twinning occurs. Hence, a higher dislocation density and larger average slip length are promoted in a large initial grain size. Therefore, the twinning stress is expected to increase with grain refinement since the slip length and dislocation density are reduced, thus making twin nucleation more difficult.

The predicted twin stress for each grain size investigated was determined to be below the bulk yield stress of the material, which is contrary to observations made by other authors [22, 18]. Bouaziz *et al.* [22] have suggested that the twin stress is not affected by the grain size and remains constant at $\sim$550 MPa. The authors further suggest that the initiation strain for twinning evolves linearly with grain size, implying that a coarser grain size requires a higher initiation strain. However, one would expect a larger grain size to promote twinning more readily since the slip length is greater. Furthermore, the model employed by Bouaziz *et al.* [22] assumes an average twin thickness which is not influenced by the initial grain size. Conversely, Gutierrez-Urrutia *et al.* [18] have reported the twin stress is strongly influenced by the yield stress which is controlled by the grain size. Consequently, the authors found that a Hall-Petch type relation provided a good estimate of the grain size on the twin stress. However, in both these studies the twin stress is conflated with the yield stress; this confusion most likely underlies the disagreement between these authors' interpretations of their data, and further, with Venables' theory [35].

The influence of grain size on the twin stress in the current experimental material indicates that the twin stress decreases with increasing grain size following a Hall-Petch type relationship, Figure 7(b). However, the calculated twin stresses are all below the yield stress of the material. Consequently, the twinning constant in a Hall-Petch type model would need to be a lower value than that required for slip. Gutierrez-Urrutia *et al.* in ref [18] have used a Hall-Petch type relationship for determining the grain size dependence on twin stress. Using the Hall-Petch constant value for twinning identical to that for slip, the authors found that the relationship overestimates the twin stress compared to experimental observations. This suggests a lower twin constant compared to slip which the experimental observations for the current TWIP steel support. This also indicates that although the twin stress increases with grain refinement, twinning is not suppressed.

A noteworthy observation is the calculated twin stress in the as-received condition 10 μm grain size material which is predicted to be ∼115 MPa. This is very similar to the stress at which deformation twinning was initiated in the same material based on X-ray synchrotron diffraction data in our complementary investigation. This is a reassuring observation, since it has been shown by the authors that deformation twins are observed in TEM foils prepared from specimens with the (111) orientation aligned to the tensile axis that have been subjected to cyclic tensile testing at 200 MPa. It has also been reported by several authors [18, 30, 40] that during the early stages of deformation in TWIP steels, twinning occurs predominantly in grains orientated close to the $\langle 111 \rangle$//tensile axis.

Once the critical stress twin nucleation is attained, any further stress only serves to thicken the already nucleated perfect f.c.c. twins. Therefore, the initial grain size is expected to influence twin morphology, whereby a larger grain size promotes the formation of thicker twins, since the twin needs to grow over a larger distance. Renard *et al.* [41] have recently shown that a greater twin thickness produces easier internal plasticity of the twins. Therefore, it would be expected that upon cyclic loading, the coarse grain material would be able to accommodate greater plastic strain per cycle since the twin thickness is assumed to be greater. As a consequence, the gradient of the line of best fit in Figures 6(a-e) would be expected to increase with grain size, which is seen in Figure 6(f).

Examination of the microstructure after each grain size material is strained to 5 % engineering strain reveals that the coarser grain material does indeed contain thicker deformation twins compared to the finer grain sizes, Figure 8. Further investigation of the finest and coarsest grain size specimens using transmission electron microscopy reinforces this observation, Figure 9. Here we can see that the relative twin thickness in the 84 μm is distinctly thicker than those observed in the 0.7 μm material even though both specimens have been deformed to the same strain. Observations from the fine grain material suggest the presence of primary twin less than 10 nm thick within the material. TEM observations also reveal a contrast in the dislocation arrangement between the fine and coarse grain samples. The the dislocation arrangement within the fine grain exhibits a relatively loose configuration and lower volume fraction compared to the coarse grain. Many of the dislocations observed in the large grain material appear to exist in dissociated pairs, Figure 9(e). The volume fraction of stacking faults observed in the two samples also appear to be affected by the grain size. A greater fraction of stacking faults were observed in the coarse grain material, Figure 9(f). Since stacking faults essentially operate as nucleation sites for twin growth, the many more faults observed within the coarse grain material may explain the lower nucleation stress required to initiate twinning in TWIP steels exhibiting larger grain sizes. The varying microstructure observations made from the fine and coarse grain samples suggest the hardening behaviour variation seen during mechanical testing is due to different twin thicknesses which is affected by the grain size.

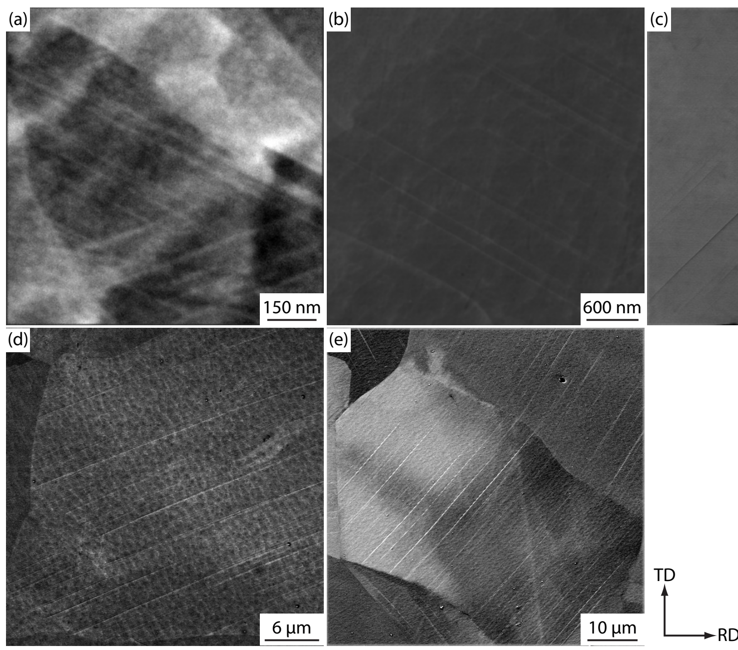

Figure 8: Backscattered electron images of the TWIP steel exhibiting different grain sizes after deformation to 5 % engineering strain showing the relative twin thickness is influenced by the initial grain size. (a) 0.7 µm, (b) 4.3 µm, (c) 10 µm, (d) 45 µm and (e) 84 µm grain size material.

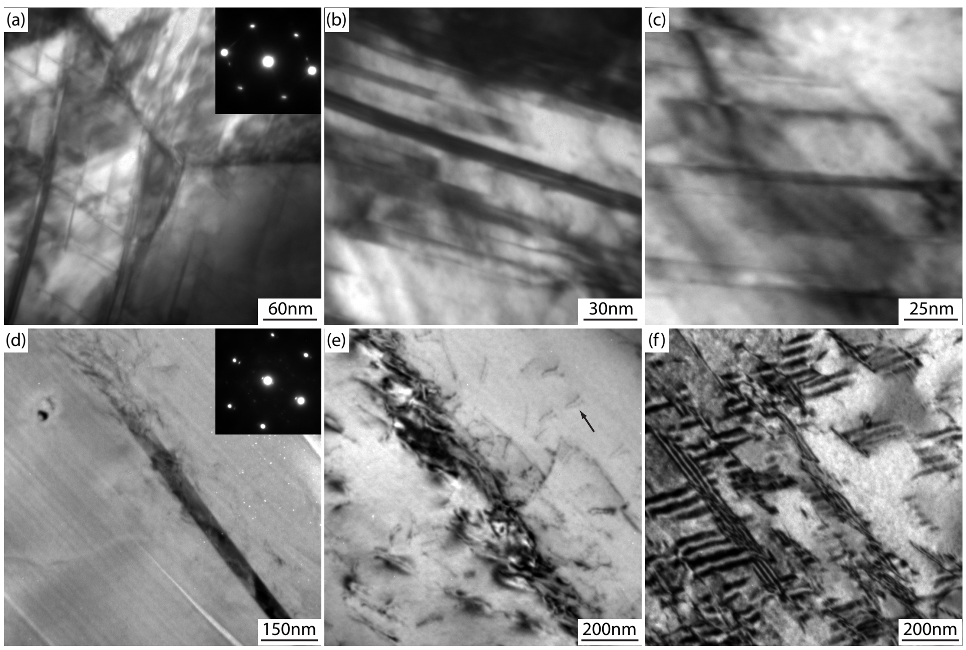

Figure 9: Bright field TEM micrographs and selected area diffraction patterns of the 0.7 μm (a-c) and 84 μm (d-f) TWIP steel after deformation to 5 % strain. The deformation twins in the fine grain material are thinner than the twins present in the coarse grain. Numerous dissociated dislocation pairs are observed in the coarse grain material as indicated by the arrow in (e). A large number of stacking faults are also present in the 84 μm grain size material (f).

4. Conclusions

The effect of initial grain size on the mechanical behaviour and microstructure of a TWIP steel have been investigated using a range of tensile testing and microscopy techniques, including transmission electron microscopy. The following conclusions can be drawn from the investigation:

1. A 15Mn-2Al-2Si-0.7C wt % TWIP steel was produced with 5 different grain sizes ranging between 0.7 - 84 μm using a combination of cold rolling and annealing.
2. The texture of the material represented a characteristic cold rolled and annealed texture comprising of Brass, Goss and Copper components. The 10 μm TWIP was obtained from the as-received condition material and has a random texture.
3. The tensile behaviour of the material showed an increase in the the yield stress with decreasing grain size. This behaviour was represented well using a Hall-Petch type relationship. Therefore grain refinement is found to result in an overall strength and energy absorption boost.
4. The strain hardening behaviour is affected by the grain size, whereby an additional hardening region is observed in the fine grained materials.
5. Cyclic tensile testing of the different grain size specimens at stresses below the yield stress revealed the accumulation of strain with each cycle. This was also used to determine the effect of grain size on the twin nucleation stress.
6. The progression of sub yield strain accumulation proceeds in a manner consistent with sub yield twinning being hardened in a conventional Hall-Petch manner.
7. The twin nucleation stress was found to increase with decreasing grain size. The critical twin stress at the single crystal limit was determined to be $\sim$50 MPa.
8. A larger amount of strain is accumulated per cycle in the coarse grain material compared to the fine grain material. It is suggested that this is due to the formation of thicker twins in the coarse grain material.
9. SEM analysis of each grain size material deformed to 5 % engineering strain revealed thicker deformation twins present in the coarser grain material.
10. TEM examination of the finest and coarsest grain size specimens reinforced the SEM observations. The dislocation arrangement was also determined to be affected by the grain size.
11. A larger fraction of stacking faults was observed in the coarse grain material indicating the relative ease for twin formation in coarse grained TWIP steels compared to a fine grain material.

5. Acknowledgements

The authors would like to thank PF Morris, M Cornelissen, PA Davies and B Berkhout from Tata steel and PM Brown from DSTL, UK for their support in useful discussions and for material supply. This work was supported from the materials and structures research programme delivered by Team MAST for the Defence Technology and Innovation Centre, part of the UK Ministry of Defence.

A. Weibull Cumulative Distribution Functions

It is common practice to plot grain size distributions from EBSD data in the form of binned histograms. However, this does not allow the easy interpretation of the grain size distribution in a statistically meaningful manner *i.e.* the mean, standard deviation or kurtosis. Furthermore, the number of grains sampled and hence the significance of any anomalies which for example may reveal a multimodal grain distribution are also unclear. Finally, the unit of the frequency axis is also often unclear, *i.e.* whether it is number or area normalised, making it difficult to compare distributions.

In the present study, we fit a distribution function to the cumulative distribution function (CDF) using a Weibull smoothing method, Figure 10(a). This allows the probability distribution to be plotted in a manner that permits the comparison between microstructures in both a visual and statistical fashion, Figure 10(b). We have chosen to use a Weibull function in the current analysis, but we acknowledge that the choice of function should ultimately be placed on a theoretically sound foundation, which would be a useful topic for further work based, *e.g.* on recrystallisation modelling [42].

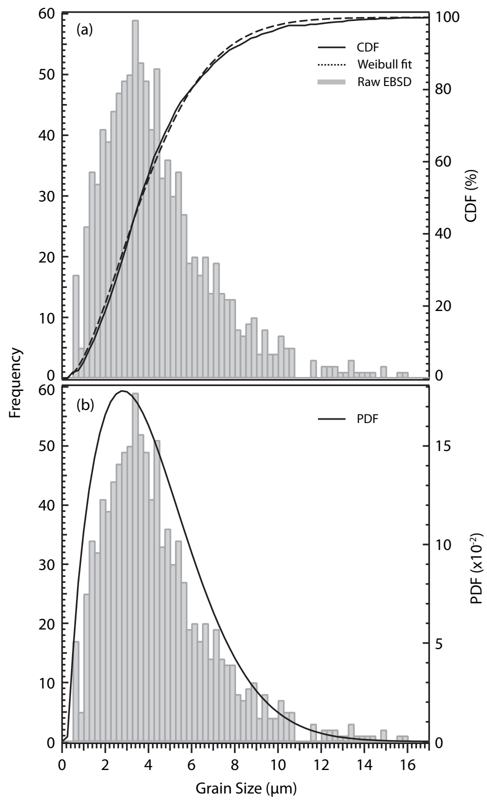

Figure 10: Weibull smoothing procedure where (a) the cumulative distribution function (CDF) of the raw EBSD data is fitted using a Weibull function and (b) smoothed probability density function (PDF) is plotted using a derivative of the fitted Weibull.

References

[1] Frommeyer G, Grassel O. Mats Sci Tech 1998;14

[2] Frommeyer G, Brux U, Neumann P. ISIJ International 2003;43:438

[3] Grassel O, Kruger L, Frommeyer G, Meyer L. International Journal of Plasticity 2000;16:1391

[4] Curtze S, Kuokkala VT. Acta Materialia 2010;58:5129

[5] Allain S, Chateau J, Bouaziz O, Migot S, Guelton N. Materials Science and Engineering A 2004;387:158

[6] Bouaziz O, Allain S, Scott CP, Cugy P, Barbier D. Current Opinion in Solid State & Materials Science 2011;15:141

[7] Idrissi H, Renard K, Ryelandt L, Schryvers D, Jacques P. Acta Materialia 2010;58:2464

[8] Guitierrez-Urrutia I, Raabe D. Scripta Materialia 2012;

[9] Venables JA. Philosophical Magazine 1974;30:1165

[10] Cohen JB, Weertman J. Acta Metallurgica 1963;11:996

[11] Mahajan S, Chin G. Acta Metallurgica 1973;21:1353

[12] Christian J, Mahajan S. Progress in Materials Science 1995;39:1

[13] Friedel J. Dislocations. Oxford, England: Pergamon Press Ltd. 1964

[14] Allain S, Chateau J, Dahmoun D, Bouaziz O. Materials Science and Engineering A 2004;387-389:272

[15] Santos DB, Saleh AA, Gazder AA, Carman A, Duarte DM, Ribeiro EAS, Gonzalez BM, Pereloma EV. Materials Science & Engineering A 2011; 528:3545

[16] Kang S, Jung YS, Jun JH, Lee YK. Materials Science & Engineering A 2010;527:745

[17] Lee TH, Oh CS, Kim SJ, Takaki S. Acta Materialia 2007;55:3649

[18] Gutierrez-Urrutia I, Zaefferer S, Raabe D. Materials Science & Engineering A 2010;527:3552

[19] Guitierrez-Urrutia I, Raabe D. Scripta Materialia 2012;66:992

[20] Dini G, Najafizadeh A, Ueji R, Monir-Vaghefi SM. Materials and Design 2010;31:3395

[21] Ueji R, Tsuchida N, Terada D, Tsuji N, Tanaka Y, Takemura A, Kunishige K. Scripta Materialia 2008;59:963

[22] Bouaziz O, Allain S, Scott C. Scripta Materialia 2008;58:484

[23] Oh B, Cho S, Kim Y, Kim Y, Kim W, Hong S. Materials Science and Engineering A 1995;197:147

[24] Bleck W, Phiu-on K, Heering C, Hirt G. Steel Research International 2007; 78:536

[25] Gallagher P. Metallurgical Transactions 1970;1:2429

[26] Matthies S, Vinel GW. Physica Status Solidi 1982;

[27] Bracke L, Verbeken K, Kestens LAI. Scripta Materialia 2012;66:1007

[28] Tsuji N, Ito Y, Saito Y, Minamino Y. Scripta Materialia 2002;47:893

[29] Barbier D, Gey N, Allain S, Bozzolo N, Humbert M. Mat Sci Eng A-Struct 2009;500:196

[30] Lebedkina TA, Lebyodkin MA, Chateau JP, Jacques A, Allain S. Materials Science and Engineering A 2009;519:147

[31] Idrissi H, Renard K, Schryvers D, Jacques PJ. Scripta Materialia 2010; 63:961

[32] Scott C, Remy B, Collet J-L, Cael A, Bao C, Danoix F, Malard B, Curfs C. Int J Mater Res 2011;102:538

[33] Fujita H, Mori T. Scripta Metallurgica 1975;9:631

[34] Venables JA. Philosophical Magazine 1961;9:379

[35] Nabarro FRN, editor. Dislocations in Solids, volume 9. Elsevier 1992; p. 135

[36] Kibey S, Liu JB, Johnson DD, Sehitoglu H. Acta Materialia 2007;55:6843

[37] Meyers MA, Vöhringer O, Lubarda VA. Acta Materialia 2001;49:4025

[38] El-Danaf E, Kalidindi SR, Doherty RD. Metallurgical and Materials Transactions A 1999;30A:1223

[39] Gutierrez-Urrutia I, Raabe D. Acta Materialia 2011;59:6449

[40] Renard K, Idrissi H, Schryvers D, Jacques PJ. Scripta Materialia 2012; 66:966

[41] Potts RB. Mathematical Proceedings of the Cambridge Philosophical Society 1952;48:106